Journal of Applied Microbiology 1998, **84**, 485–492

Characterization of axenic *Pseudomonas fragi* and *Escherichia coli* biofilms that inhibit corrosion of SAE 1018 steel

A. Jayaraman, A.K. Sun and T.K. Wood

Department of Chemical and Biochemical Engineering & Materials Science, University of California, Irvine, CA, USA

6061/01/97: received 13 January 1997, revised 4 June 1997 and accepted 9 June 1997

A. JAYARAMAN, A.K. SUN AND T.K. WOOD. 1998. Corrosion inhibition of SAE 1018 steel by *Pseudomonas fragi* and *Escherichia coli* biofilms has been evaluated using batch cultures in rich medium (LB) and seawater-mimicking medium (VNSS) at 23 °C and 30 °C with or without daily medium replenishment. Biofilm components have been stained simultaneously for polysaccharide (calcofluor) and live and dead cells (Live/Dead *Bac*lit viability kit) and visualized using confocal scanning laser microscopy (CSLM). Image analysis was used to quantify the relative proportions of live cells, dead cells, polysaccharide and void space in the biofilm. This staining technique and examination of the architecture of biofilms responsible for inhibiting metal corrosion revealed that both *Ps. fragi* and *E. coli* produce polysaccharide only in the seawater medium; in rich medium, the biofilm consisted mainly of a layer of sessile cells near the biofilm–metal interface and sparse thick clumps of cells at the biofilm–liquid interface. Biofilms of both strains had a higher proportion of live cells in the rich medium than in the seawater-mimicking medium at the higher temperature, and more live cells were present at the higher temperature for LB medium. The corrosion inhibition observed (2·3–6·9-fold in 8 d) was not significantly affected by medium type or replenishment. Increase in the cellular content of the biofilms, as a result of increasing temperature, led to a reduction in corrosion.

INTRODUCTION

Biofilms are adherent microbial populations that are trapped in an exopolysaccharide matrix (Hoyle *et al.* 1990). Metabolically active bacteria exhibit an increased tendency to attach to surfaces and based on the availability of nutrients, produce exopolymers to form mature biofilms (Costerton *et al.* 1995). The exopolysaccharide helps in the adhesion of bacteria to the surface and for further bacterial accumulation in the biofilm (Beech and Gaylarde 1991; Costerton *et al.* 1995). Both *Pseudomonas fragi* (Parolis *et al.* 1991) and *Escherichia coli* (Huang *et al.* 1994) are known to produce exopolysaccharides and form such biofilms.

Biofilms are not formed randomly but are structured as a response to the surrounding environment, nutrient conditions, and metabolic processes (Lawrence *et al.* 1991). Pure culture and multispecies biofilms form complex structures with non-uniform distribution of clusters of cells, and water channels or voids (de Beer *et al.* 1994). The highly hydrated nature of the biofilms requires a non-invasive tool like confocal scanning laser microscopy (CSLM) for analysis (Shotton and White 1989); CSLM permits the non-destructive analysis of biofilms in real time, eliminates the interference from out-of-focus planes, requires no chemical fixing steps, and permits sectioning of the biofilm in both horizontal and sagittal orientations to give detailed information on the composition of multispecies biofilms, the cell morphology and physiology, metabolic state, and biofilm architecture (Lawrence *et al.* 1991; Costerton *et al.* 1994, 1995).

Biofilms can cause significant losses to industry by fouling ship hulls, cooling towers and pipes (Bryers 1987; Blenkinsopp and Costerton 1991). On the other hand, *Pseudomonas* and other aerobic biofilms have been shown to change the rate of metal corrosion (Nivens *et al.* 1986; Black *et al.* 1988). Jayaraman *et al.* (1997b, c) and Pedersen and Hermansson (1989, 1991) have also reported the inhibition of corrosion with pseudomonads and other aerobic bacteria.

Correspondence to: Professor T.K. Wood, Department of Chemical and Biochemical Engineering & Materials Science, University of California, Irvine, CA 92697–2575, USA (e-mail: tkwood@uci.edu).

In this study, axenic *Ps. fragi* and *E. coli* DH5α (pKMY319) biofilms were developed on metal coupons and also inhibited corrosion. The main objectives of this study were to characterize the protective biofilm architecture and correlate the biofilm constituents to corrosion inhibition. Biofilms were stained for live cells, dead cells and exopolysaccharide, visualized using CSLM, and quantified to obtain depth profiles. The effect of increasing temperature and growth medium salt content, both on the biofilm composition and corrosion inhibition, was studied.

MATERIALS AND METHODS

Bacterial strains, growth media and culture conditions

A kanamycin-resistant, transposon mutant of the spoiled-meat bacterium *Ps. fragi* ATCC 4973 (*Ps. fragi* K) (Jayaraman *et al.* 1997a) and a tetracycline-resistant enteric bacterium, *E. coli* DH5α (pKMY319) (Jayaraman *et al.* 1997a) were used, based on their ability to form biofilms (Parolis *et al.* 1991; Huang *et al.* 1993). Both strains were cultivated without shaking at 23 °C or 30 °C in 250 ml Erlenmeyer flasks with multiple SAE 1018 metal coupons in 35 ml of Luria-Bertani medium (LB, Maniatis *et al.* 1982) and Vaatanen nine salts solution (VNSS, Hernandez *et al.* 1994) supplemented with 50 μg ml^{-1} of kanamycin (Jayaraman *et al.* 1997a) or 25 μg ml^{-1} of tetracycline (Yen 1991). All strains were streaked from a −85 °C glycerol stock onto LB agar plates with appropriate antibiotics. A single colony was then picked and used to inoculate 10 ml of growth medium, with suitable antibiotics, and grown overnight at 30 °C, 250 rev min^{-1} (New Brunswick Scientific, Edison, NJ, USA; series 25 shaker). A 0·1% inoculum (350 μl) was used for developing biofilms for the corrosion experiments. Medium replenishment was by slow removal of the old medium and gentle addition of fresh medium along the walls of the Erlenmeyer flask.

Metal coupon preparation and mass loss determination

SAE 1018 steel coupons weighing 5·1 g and having a diameter of 25·5 mm and a thickness of 1·2 mm were cut from sheet stock, polished with 240 grit polishing paper (Buehler, Lake Bluff, IL, USA) and prepared as reported previously (Jayaraman *et al.* 1997a). The specific mass loss observed (mg cm^{-2}) was determined by dividing by the total surface area of the coupon (11·18 cm^2) and was used as an indicator of the extent of corrosion (Jayaraman *et al.* 1997a). All corrosion experiments were performed with three replicates.

Confocal scanning laser microscopy (CSLM) and determination of biofilm thickness

Metal coupons with attached surface biofilms were removed from Erlenmeyer flasks and immersed once in 0·85% NaCl to remove bulk supernatant cells. Cells and polysaccharide were stained for 30 min simultaneously in 4 ml of staining solution using the Live/Dead *Bac*lit bacteria viability assay kit protocol (1·125 μl ml^{-1}of each stain component; Molecular Probes, Eugene, OR, USA) and calcofluor (300 μg ml^{-1}; Sigma, St Louis, MO, USA, Stewart *et al.* 1995). The Live/Dead viability kit distinguishes live and dead cells based on membrane integrity; live cells with intact membranes stain green, and dead cells with compromised membranes stain red. The stained coupons were transported to the stage of a confocal scanning laser microscope (MRC 600, Bio-Rad, Hercules, CA, USA) equipped with a krypton/argon laser, and a 60×, 1·4 NA oil-immersion lens. To minimize the damage to the biofilm when placed on the stage of the inverted microscope, a 1·8 cm diameter coverslip (circles no. 1, 0·13–0·17 cm thick, Fisher Scientific Co., Pittsburgh, PA, USA) was gently placed on the coupon (held by capillary action), and the coupon (2·55 cm diameter) was held by the circular microscope aperture (2·0 cm diameter) in the area outside the coverslip. The central area of the biofilm was not compressed by the weight of the coupon and only this area was visualized. The sample was excited at 488 nm, and the fluorescent light was imaged using the K1/K2 filter block combination. The biofilms shown in Fig. 1 were analysed using an MRC 1024 confocal microscope (Bio-Rad) with a T1/E2 multipurpose filter combination. Thin optical sections (horizontal sectioning) of 0·5–1·0 μm were collected over the complete biofilm thickness for a representative position (chosen as one of four similar positions in the biofilm on the same coupon). The biofilm thickness was found by focusing on the top and bottom of a biofilm with the distance travelled corrected for refractive index (Bakke and Olsson 1986), and the thickness was determined as the average of the four similar positions analysed on the same coupon.

Image analysis

Image processing and analysis of all biofilms were performed with the COMOS software available on the Bio-Rad MRC600. Optical sections were discriminated based on pixel intensities to differentiate live and dead cells, polysaccharide and void space. The percentage of each section area covered by a range of pixel intensities was then measured to obtain the relative proportions of the component in each section; these relative proportions of each component were plotted as a function of the normalized depth (depth at which the image was obtained divided by the total biofilm thickness). Accord-

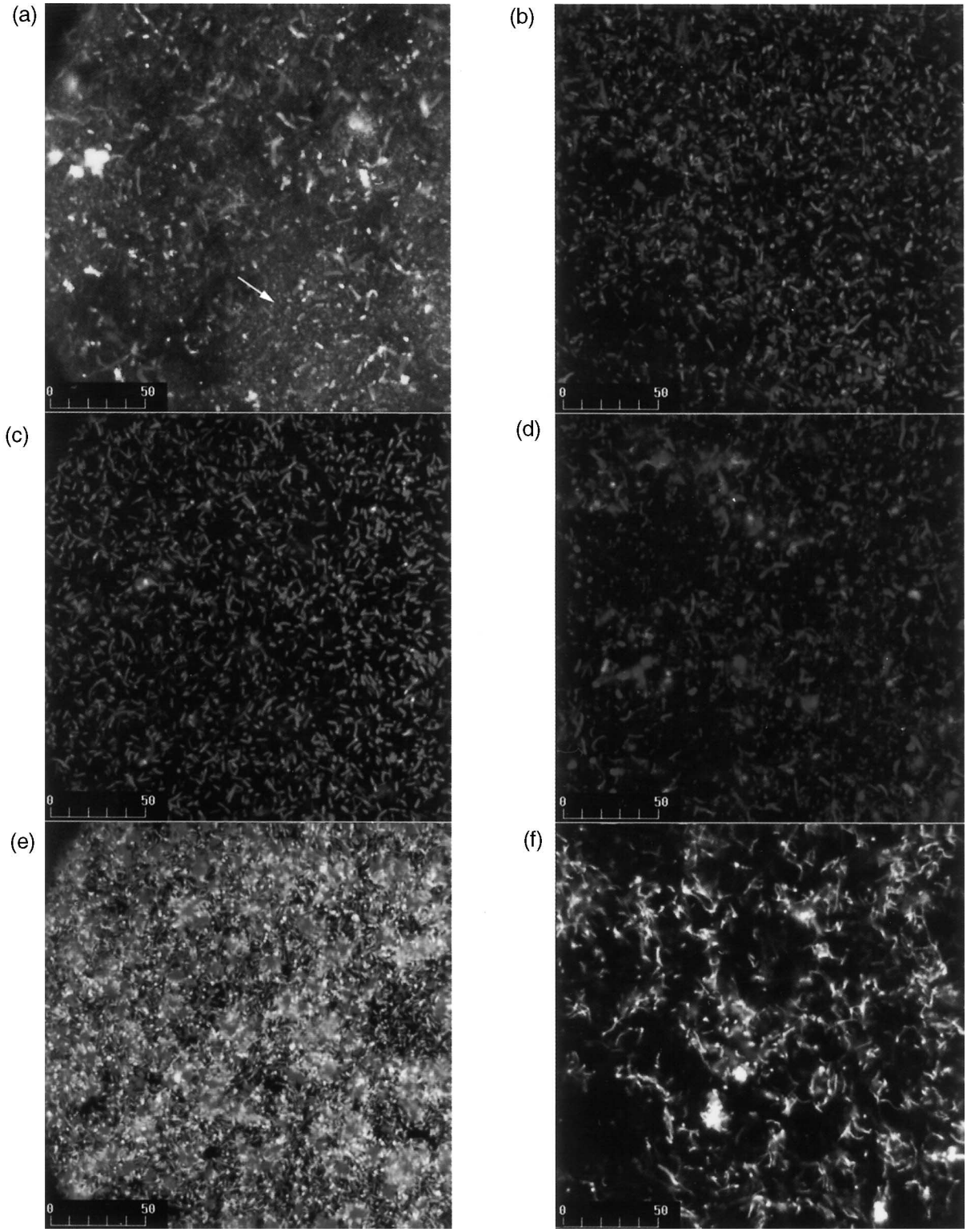

Fig. 1 Confocal scanning microscope (MRC 1024) images of 4-day batch culture biofilms on SAE 1018 steel. (a) *Escherichia coli* DH5α (pKMY319) in VNSS medium at 30 °C with daily medium replenishment, stained for cells and polysaccharide, normalized depth = 0·70; arrow indicates polysaccharide; (b) *E. coli* DH5α (pKMY319) in LB medium at 30 °C with daily medium replenishment, stained for cells and polysaccharide, normalized depth = 0·70; (c) *E. coli* DH5α (pKMY319) in LB medium at 30 °C with no medium replenishment, stained for cells alone, normalized depth = 0·80; (d) *Pseudomonas fragi* K in LB medium at 23 °C with no medium replenishment, stained for cells alone, normalized depth = 0·85; (e) *Ps. fragi* K in LB medium at 30 °C with no medium replenishment, stained for cells alone, normalized depth = 0·90; (f) *Ps. fragi* K in VNSS medium at 30 °C with no medium replenishment, stained for cells alone, normalized depth = 0·90. Scale bar represents 50 μm

ingly, position 0·0 represents the biofilm–liquid interface and position 1·0 represents the biofilm–metal interface.

RESULTS

Corrosion inhibition with *Ps. fragi* and *E. coli*

Mass loss in LB medium and VNSS medium with *Ps. fragi* K or *E. coli* DH5α (pKMY319) was examined for 8 d in stationary batch cultures at 23 °C and 30 °C in which the growth medium was either replenished daily or left unchanged for 8 d. The metal coupons immersed in bacterial suspensions showed a 2·3–6·9-fold decrease in mass loss after 8 d compared with coupons immersed in sterile media (Table 1). These results compare well with those of Jayaraman *et al.* (1997a) and Pedersen and Hermansson (1989) who reported an eightfold reduction in corrosion of SIS 1146 steel using *Pseudomonas* S9 and *Serratia marscens* after 19 days of exposure in VNSS medium. Previous work in this laboratory has shown that there is no difference in the corrosion of SAE 1018 steel coupons in sterile, fresh LB medium and spent, filtered LB medium (Jayaraman *et al.* 1997a).

The 8-day mass loss observed with *Ps. fragi* K and *E. coli* DH5α varied with the growth medium and the cultivation temperature. The total mass lost was less at the lower temperature for both media; however, corrosion inhibition (as a percentage reduction in mass loss of the sterile control) was comparable or higher at the higher temperature in both media. Table 1 shows that the mass loss with both strains at both temperatures was less in LB medium compared with VNSS medium. Daily replenishment of the medium did not significantly affect corrosion inhibition except with *Ps. fragi*

Table 1 Four-day *Pseudomonas fragi* K batch culture biofilm values chosen as representative from one of four positions viewed at the same depth from a single coupon. The normalized depth position in the biofilm which is indicated corresponds to the approximate maximum cellular content (live and dead cells), and the % live cells, % dead cells, % EPS, and % void listed at this position are from COMOS data analysis (MRC 600 microscope)

		Normalized depth	% live cells	% dead cells	% EPS	% void	Thickness (μm)	Corrosion* (mg cm^{-2})
LB 23 °C	Sterile medium, replenished	—	—	—	—	—	—	0·54 ± 0·08
	Sterile medium	—	—	—	—	—	—	0·45 ± 0·03
	Ps. fragi K; replenished	0·60	12	19	< 3	66	13	0·13 ± 0·02
	Ps. fragi K	0·80	40	10	< 3	49	18	0·11 ± 0·02
	E. coli DH5α; replenished	0·60	18	5	10	67	13	0·21 ± 0·03
	E. coli DH5α	0·90	29	9	< 3	60	11	0·17 ± 0·03
LB 30 °C	Sterile mediums replenished	—	—	—	—	—	—	1·13 ± 0·18
	Sterile medium	—	—	—	—	—	—	1·03 ± 0·15
	Ps. fragi K; replenished	0·60	39	31	< 3	27	13	0·15 ± 0·02
	Ps. fragi K	0·90	50	46	< 3	< 5	17	0·20 ± 0·02
	E. coli DH5α; replenished	0·80	35	30	< 3	35	19	0·23 ± 0·04
	E. coli DH5α	0·90	12	53	< 5	35	16	0·18 ± 0·02
VNSS 23 °C	Sterile medium, replenished	—	—	—	—	—	—	0·65 ± 0·07
	Sterile medium	—	—	—	—	—	—	0·62 ± 0·07
	Ps. fragi K; replenished	0·80	13	27	26	52	10	0·18 ± 0·02
	Ps. fragi K	0·80	5	3	20	73	12	0·16 ± 0·01
	E. coli DH5α; replenished	0·70	18	12	31	38	11	0·28 ± 0·02
	E. coli DH5α	0·90	18	12	40	30	11	0·24 ± 0·02
VNSS 30 °C	Sterile medium, replenished	—	—	—	—	—	—	1·20 ± 0·12
	Sterile medium	—	—	—	—	—	—	1·37 ± 0·15
	Ps. fragi K; replenished	0·80	26	21	11	42	16	0·20 ± 0·03
	Ps. fragi K	1·0	15	9	55	21	16	0·53 ± 0·09
	E. coli DH5α; replenished	0·70	16	14	51	21	14	0·32 ± 0·04
	E. coli DH5α	0·70	7	32	10	51	15	0·50 ± 0·03

* 8-day corrosion values.

K in VNSS medium at 30 °C where corrosion inhibition was nearly 2·3-fold better (Table 1). Irrespective of medium replenishment, *E. coli* DH5α (pKMY319) resulted in a higher mass loss than *Ps. fragi* K at 23 °C, and the mass loss in the presence of both strains was comparable at 30 °C. Sterile controls corroded to the same extent irrespective of whether the medium was replaced daily (Table 1).

Metal coupons in most suspensions of bacteria corroded at a rate of approximately 0·03–0·06 mg cm^{-2} day^{-1} during the first 4 d. The corrosion rate decreased beyond 4 d. Sterile controls corroded at a slightly faster rate in VNSS medium than in LB medium at both temperatures (Table 1), and the corrosion rate was relatively uniform for the entire 8-day period.

Determination of biofilm thickness by CSLM

Multiple coupons were removed from the medium after 2, 3, 4 and 8 d, stained for cells and polysaccharide simultaneously, and analysed by CSLM. Biofilms observed under 100 × magnification (no coverslip) and 600 × magnification (with coverslip) showed a similar depth profile of live and dead cells and polysaccharide (not shown). However, it was not possible to compare accurately the biofilm thickness obtained with and without a coverslip because the 10 × (0·6 NA) objective lens uses a thicker optical section and results in an over-estimate of the true thickness as rejection of out-of-focus information is proportional to the square of the numerical aperture (Keller 1990).

Both *Ps. fragi* K and *E. coli* DH5α (pKMY319) biofilms developed to a detectable thickness (approximately 10–15 μm) within the first 48 h of exposure to growth media (data not shown). *Pseudomonas fragi* K biofilms did not vary significantly in thickness for different growth temperatures, media and medium replenishment, and the biofilm was approximately 14 μm thick after 4 d (Table 1); the biofilm thickness was approximately 12 μm after 8 d of exposure (not shown). *Escherichia coli* DH5α (pKMY319) exhibited a similar trend, with a 4-day biofilm (13 μm, Table 1) being slightly thicker than an 8-day biofilm (approximately 11 μm, not shown).

Characterization of the biofilms

Pseudomonas fragi K and *E. coli* DH5α (pKMY319) biofilms in LB and VNSS medium with and without medium replenishment at 23 and 30 °C were characterized and analysed using image analysis to create 4-day normalized depth profiles. Although the micrographs in Fig. 1 are at different distances from the metal surface, they are all at approximately the same normalized spatial position in the respective biofilms. Data from analysis of all biofilms are not shown for reasons of brevity; an analysis from *one* representative position at a single depth for all the biofilms (where the cellular content was near maximum) is shown in Table 1, and analysis from *all* depths at one representative position for *one* bacterium (*Ps. fragi* K) at one temperature (30 °C) and both media is shown in Figs 2 and 3.

As a control experiment to verify that the Live/Dead stain can be used to quantify populations with live and dead cells, 200 μg ml^{-1} of kanamycin was added to a 12 h wild-type *Ps. fragi* culture and visualized with CSLM after 48 h. The sample was predominantly red (approximately 75%, data not shown), with a few green and yellow cells. The biofilm sample was also streaked on LB agar plates and minimal growth was observed along the main streak path (whereas cells not exposed to antibiotic grew as a bacterial lawn along the main streak). Hence, the stain can be used for identifying and quantifying dead cells.

Horizontal sections at each 1·0 μm of depth of *Ps. fragi* K and *E. coli* DH5α (pKMY319) biofilms were obtained with

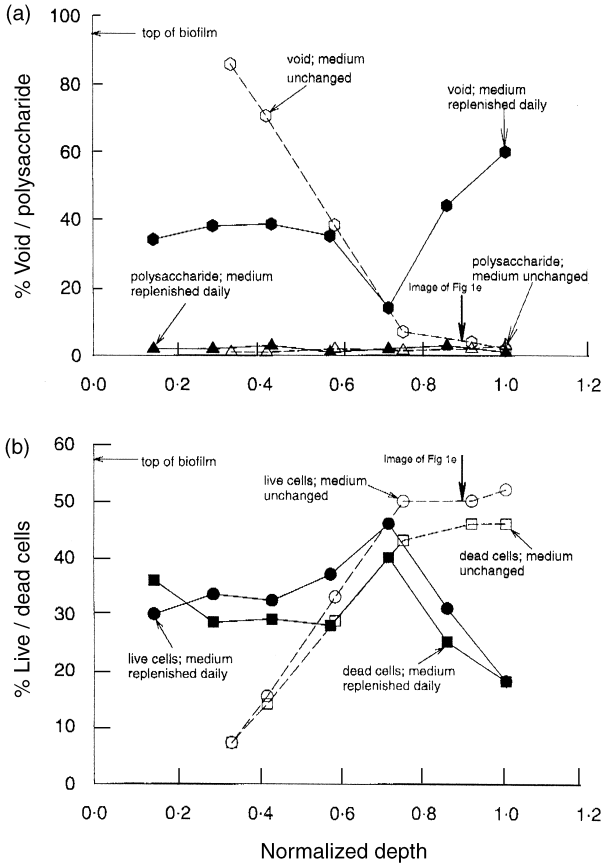

Fig. 2 Depth profiles of 4-day, batch-culture, *Pseudomonas fragi* K biofilms developed on SAE 1018 steel with or without medium replenishment in LB medium at 30 °C. Measurements are of a representative position in the biofilm (one of four viewed). Arrow indicates position where image from Fig. 1e was obtained

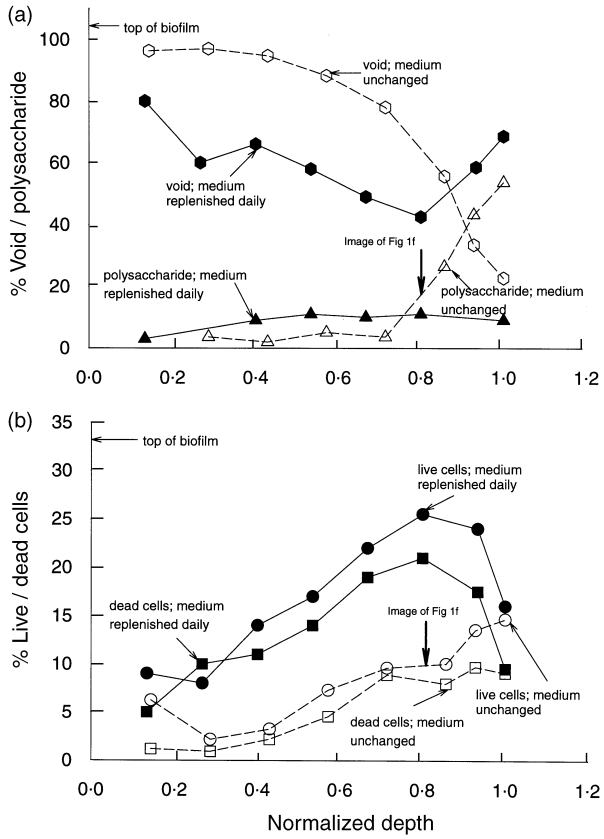

Fig. 3 Depth profiles of 4-day, batch culture, *Pseudomonas fragi* K biofilms developed on SAE 1018 steel in VNSS medium with or without medium replenishment at 30 °C. Measurements are of a representative position in the biofilm (one of four viewed). Arrow indicates position where image from Fig. 1f was obtained

the confocal microscope, and the distribution of live cells, dead cells, exopolysaccharide (EPS) and void spaces were determined. Both *Ps. fragi* K and *E. coli* DH5α (pKMY319) biofilms consisted of uniform layers of cells and polysaccharide (whenever present) near the metal surface. The ratio of cellular (live and dead cells) to non-cellular matter (polysaccharide and water channels) varied with depth for all biofilms. Biofilms of both strains exhibited a pyramidal architecture, with a dense concentration of cells near the bottom of the biofilm (biofilm–metal interface) and a sparse distribution of cells near the biofilm–liquid interface (Figs 2 and 3). This is in agreement with Lawrence *et al.* (1991) who reported a similar pyramidal structure for *Ps. fluorescens* and *Ps. aeruginosa* biofilms developed on glass slides in complex and minimal media with continuous cultures. In the present work, the top layers of the biofilm predominantly consisted of live cells, and the live-cell density decreased near the metal surface. Polysaccharide (when present) was usually detected near the bottom of the biofilm (typically at 3 μm from the metal surface). Thick clumps of loosely associated live and dead cells (15–40 μm thick) were present at the top of the biofilm (at the biofilm–liquid interface) and were not considered for determination of biofilm thickness. *Escherichia coli* DH5α (pKMY319) biofilms also had a thin layer of slime covering the metal coupons after 8 d of exposure to growth medium which could not be retained on top of the metal coupon during the staining procedure.

The *Ps. fragi* K 4-day depth profiles in LB and VNSS medium at 30 °C are shown (Figs 2 and 3), and are representative of the general trends observed under other conditions and with *E. coli*. More cells were detected in *Ps. fragi* K and *E. coli* DH5α biofilms grown in LB medium than in VNSS medium at 30 °C (Table 1, Fig. 1e and 1f, Figs 2 and 3). Furthermore, more cell mass was formed with *Ps. fragi* at higher temperatures in LB medium since at 23 °C, 50% of the biofilm was made up of live and dead cells (Table 1), whereas biofilms grown at 30 °C had 90% live and dead cells (Table 1). In biofilms developed in VNSS medium, polysaccharide accounted for nearly 10–55% of the biofilm (Table 1) whereas in LB medium, less than 5% EPS was detected.

By replacing the medium daily, the relative proportions of the biofilm constituents changed significantly (Figs 2 and 3); typically, more live cells were detected in the biofilm with medium replenishment under all conditions (Fig. 1b and 1c and not shown) although this trend is not evident from the analysis of the single positions shown in Table 1. The biofilm architecture also changed with the addition of fresh medium daily with nearly equal proportions of cells observed at all depths of the biofilm instead of a pyramidal architecture. The ratio of cellular material to non-cellular material remained relatively constant throughout the biofilm for most conditions (Figs 2b and 3b), and polysaccharide was observed only in VNSS medium (Fig. 1a and 1b). The extent of polysaccharide production (whenever present) was greater with medium replenishment (Figs 2a and 3a and Table 1). Less clumping was observed at the upper layers of the biofilm, and the proportion of live cells also did not decrease significantly towards the bottom of the biofilm.

DISCUSSION

CSLM image analysis of the biofilms, and quantification of the relative proportions of live cells, dead cells, EPS and void space revealed that the maximum cell (live and dead) density was obtained after four days of exposure and decreased beyond four days (data not shown). Therefore, 4-day batch culture biofilms of *Ps. fragi* K and *E. coli* DH5α (pKMY319) grown on metal coupons in LB medium and VNSS medium were selected for further characterization and comparison with 4-day biofilms grown with daily medium replenishment.

The composition of the biofilms depended on the growth medium, temperature of cultivation, and medium replenishment. Development of biofilms in LB medium beyond 4 d showed a decrease in cell number, suggesting that the absence of a polysaccharide matrix causes detachment of cells (not shown). In VNSS medium, the cells were embedded in a polysaccharide matrix and showed a lesser tendency to detach from the metal surface on exposure beyond 8 d (not shown). This compares well with Dewanti and Wong (1995) who observed a similar biofilm structure with *E. coli* O157:H7 grown in trypticase soy broth and minimal media. Further, the physiology and cell morphology of the biofilm bacteria were different in biofilms developed in different media and temperatures. *Pseudomonas fragi* and *E. coli* biofilms developed in LB medium were observed as small and distinct cells; in contrast, biofilms in VNSS medium were elongated and in clusters, probably as a response to environmental stress.

Replenishing the growth medium daily caused a small decrease in the cellular content throughout the depth of the biofilm and less clumping was observed (not shown). The continuous availability of nutrients could possibly enhance the attachment of metabolically active cells to the biofilm, causing addition of cells at the top of the biofilm to replace lost cells, and is consistent with the observations of Costerton *et al.* (1995). The absence of clumping at the biofilm–liquid interface could also be explained by the minimal disturbance to the biofilm architecture caused by the daily addition of fresh growth medium and the staining procedure.

The characteristics of the biofilms (discerned through CSLM), when compared with the corrosion results, indicate that increasing the total cells in the biofilm increases corrosion inhibition. Increasing the temperature from 23 °C to 30 °C results in a 100% increase in corrosion for the sterile controls and a 1·6–4·1-fold increase in cell mass (calculated as the average total live and dead cells along the *entire* depth profile of the biofilm) for six of the eight conditions studied (two bacteria, two media and two temperatures). Corresponding to this increase in cell mass and temperature, there was only a 22% increase in corrosion for six of eight biofilm conditions (for *E. coli* DH5α in VNSS medium with daily replenishment, corrosion increased 100%; and for *Ps. fragi* K in VNSS medium without replenishment, corrosion increased 230%). Hence, in general, increasing temperature increased cell mass, and the increase in corrosion for coupons protected by biofilms was much less than that seen with sterile media (22% *vs* 100%).

Previous work in this laboratory on corrosion inhibition with seven widely varying bacterial genera (with differing degrees of biofilm formation) confirm that a homogeneous biofilm is necessary (Jayaraman *et al.* 1997b); metal coupons exposed to bacterial suspensions of *Streptomyces* (which formed a sparse biofilm with cells distributed in clumps) corroded at a rate comparable to sterile controls. However, as the ratio of corrosion in this study after 4 d with *Ps. fragi* to corrosion in a similar sterile control is comparable at 23 °C and 30 °C with LB medium and VNSS medium, similar corrosion inhibition is afforded by the biofilm even though the thickness, composition, and characteristics of the biofilm under the four conditions are drastically different. Hence, it appears that a certain minimum biofilm thickness or density is required for corrosion inhibition. Similar results occurred with *E. coli* in VNSS medium at 30 °C.

When the growth medium was replenished daily, it was interesting to note that significant differences in corrosion inhibition were seen only in VNSS medium at 30 °C (Table 1). Apart from increasing or decreasing the thickness of the biofilm, one of the main differences seen by replenishing the medium was the increase in the uniformity of the distribution of cells throughout the biofilm and an increase in the relative proportion of live cells (Figs 2b and 3b). This uniform layer of cells could reduce the amount of oxygen available at the metal surface for the corrosion process, and thereby inhibit corrosion. The lack of a significant change in corrosion inhibition compared with not replenishing the medium for other conditions also suggests an upper limit for corrosion inhibition by a particular bacterium which is quickly reached in a uniform biofilm by a minimum number of actively respiring cells.

ACKNOWLEDGEMENTS

This work was supported by a grant from the Electric Power Research Institute (Award RP8044–02). The authors would also like to thank Prof. J. D. Lipscomb for providing *E. coli* DH5α (pKMY319) and Susan D. DeMaggio for assistance with confocal microscopy.

REFERENCES

Bakke, R. and Olsson, P.Q. (1986) Biofilm measurements by light microscopy. *Journal of Microbiological Methods* **20,** 219–224.

Beech, I.B. and Gaylarde, C.C. (1991) Microbial polysaccharides and corrosion. *International Biodeterioration* **27,** 95–107.

de Beer, D., Stoodley, P., Roe, F. and Lewandowski, Z. (1994) Effects of biofilm structures on oxygen distribution and mass transport. *Biotechnology and Bioengineering* **43,** 1131–1138.

Black, J.P., Ford, T.E. and Mitchell, R. (1988) Corrosion behavior of metal-binding exopolymers from iron- and manganese-depositing bacteria. Presented at Corrosion 88, Houston, Texas.

Blenkinsopp, S.A. and Costerton, J.W. (1991) Understanding bacterial biofilms. *Trends in Biotechnology* **9,** 138–143.

Bryers, J.D. (1987) Biologically active surfaces: processes governing the formation and persistence of biofilms. *Biotechnology Progress* **3,** 57–67.

Costerton, W.J., Lewandowski, Z., Caldwell, D.E., Korber, D.R.

and Lappin-Scott, H.M. (1995) Microbial biofilms. *Annual Review of Microbiology* **49,** 711–745.

Costerton, W.J., Lewandowski, Z., DeBeer, D., Caldwell, D., Korber, D. and James, G. (1994) Biofilms, the customized microniche. *Journal of Bacteriology* **176**, 2137–2142.

Dewanti, R. and Wong, A.C.L. (1995) Influence of culture conditions on biofilm formation by *Escherichia coli* O157:H7. *International Journal of Food Microbiology* **26**, 147–164.

Hernandez, G., Kucera, V., Thierry, D., Pedersen, A. and Hermansson, M. (1994) Corrosion inhibition of steel by bacteria. *Corrosion* **50**, 603–608.

Hoyle, B.D., Jass, J. and Costerton, J.W. (1990) The biofilm glycocalyx as a resistance factor. *Journal of Antimicrobial Chemotherapy* **26,** 1–6.

Huang, C.-T., Peretti, S.W. and Bryers, J.D. (1993) Plasmid retention and gene expression in suspended and biofilm cultures of recombinant *Escherichia coli* DH5α (pMJR1750). *Biotechnology and Bioengineering* **41**, 211–220.

Huang, C.-T., Peretti, S.W. and Bryers, J.D. (1994) Effects of medium carbon-to-nitrogen ratio on biofilm formation and plasmid stability. *Biotechnology and Bioengineering* **44**, 329–336.

Jayaraman, A., Cheng, E.T., Earthman, J.C. and Wood, T.K. (1997b) Importance of biofilm formation for corrosion inhibition of SAE 1018 steel by axenic culture aerobic biofilms. *Journal of Industrial Microbiology* **18**, 396–401.

Jayaraman, A., Cheng, E.T., Earthman, J.C. and Wood, T.K. (1997c) Axenic aerobic biofilms inhibit corrosion of SAE 1018 steel through oxygen depletion. *Applied Microbiology and Biotechnology* **48**, 11–17.

Jayaraman, A., Earthman, J.C. and Wood, T.K. (1997a) Corrosion inhibition by aerobic biofilms on SAE 1018 steel. *Applied Microbiology and Biotechnology* **47,** 62–68.

Keller, H.E. (1990) Objective lenses for confocal microscopy. In *Handbook of Biological Confocal Microscopy* ed. Pawley, J.B. pp. 77–86. New York: Plenum Press.

Lawrence, J.R., Korber, D.R., Hoyle, B.D., Costerton, J.W. and Caldwell, D.E. (1991) Optical sectioning of microbial biofilms. *Journal of Bacteriology* **173,** 6558–6567.

Maniatis, T., Fritsch, E.F. and Sambrook, J. (1982) *Molecular Cloning: A Laboratory Manual.* Cold Spring Harbor, NY: Cold Spring Harbor Laboratory Press.

Nivens, D.E., Nichols, P.D., Henson, J.M., Geesey, G.G. and White, D.C. (1986) Reversible acceleration of the corrosion of AISI304 stainless steel exposed to seawater induced by growth of the marine bacterium *Vibrio natriegens. Corrosion* **42,** 204–210.

Parolis, L.A.S., Parolis, H., Dutton, G.G.S., Wing, P.L. and Skura, B.J. (1991) Structure of the glycocalyx polysaccharide of *Pseudomonas fragi* ATCC 4973. *Carbohydrate Research* **216,** 495–504.

Pedersen, A. and Hermansson, M. (1989) The effects on metal corrosion by *Serratia marscens* and a *Pseudomonas* sp. *Biofouling* **1,** 313–322.

Pedersen, A. and Hermansson, M. (1991) Inhibition of metal corrosion by bacteria. *Biofouling* **3,** 1–11.

Shotton, D. and White, N. (1989) Confocal scanning microscopy: three-dimensional biological imaging. *Trends in Biochemical Sciences* **14,** 435–439.

Stewart, P.S., Murga, R., Srinivasan, R. and DeBeer, D. (1995) Biofilm structural heterogeneity visualized by three microscopic methods. *Water Research* **29,** 2006–2009.

Yen, K.-M. (1991) Construction of cloning cartridges for development of expression vectors in Gram-negative bacteria. *Journal of Bacteriology* **173,** 5328–5335.